Synthesis, Characterization and In Vitro Antibacterial Activities of Some Amino Acids Functionalized Nanoclays from Two Local Deposits

U.U. Elele[1], Azeh Yakubu[2*], Bala Ezekiel[3], Alfred Gimba[4]

[1,2,4]*Department of Chemistry, Ibrahim Badamasi Babangida University, Lapai, Nigeria.*

[3]*Department of Microbiology, Ibrahim Badamasi Babangida University, Lapai, Nigeria*

**Corresponding author*

Abstract*- Nanoclay was synthesized by hydration of local clay deposit samples, functionalized and characterized using Raman Spectroscopy, Thermogravimetry, Brunauer Emmett Teller (BET) and Particle sizer. Samples were studied for their mineral types and in vitro antibacterial activities. The results proved significant for the classification of the studied clay deposits into natural healing or non-healing clays. Modification of nanoclay conferred antibacterial properties against clinical isolates: Escherichia Coli (E. Coli), Pseudomonas aeroginosa1 (Wound swab), Pseudomonas aeroginosa2 (Ear Swab), Staphylococcus aureus and Proteus Sp. Findings of the study showed that nanoclay was successfully synthesized as revealed by the pore width and volume in the range of 0.03675-5.349 nm and 0.03352-0.0914 cm^3/g, with a BET surface area of 432.6 m^2/g for the control sample (DNCC). Whereas Arginine/phenylalanine modified nanoclay had 0.03675-5.3490 nm and 0.005877-0.04399 cm^3/g each with a BET SA of 102.1 m^2/g and 310.3 m^2/g respectively. The surface coverage by the two different organo-cations (Arg^+, Phe^+) were 76.4 and 28.3 % respectively. Study revealed that the deposits were composed of a mixture of clay minerals (quartz, crystallite, tridymite and opal, feldspar, hematite, Kaolinite and Illite). Absorption peak around 1774-1784 cm^{-1} was due to C=O stretch. The peak around 801-820 cm^{-1} was due to modification. Degradation temperature range was from 450-800 ^oC. The novelty in this that the Nigerian clay sample from the Dogon-ruwa deposit exhibited no in vitro antibacterial activities. However, modification hugely enhanced the degree of antibacterial activities of the nanoclay. While Kaffin-koro nanoclay exhibited in vitro antibacterial activities and these were enhanced due to modification with amino acids. The study demonstrates that modification with appropriate organic cations could increase the antibacterial robustness of the studied clay deposits for useful biological applications.

Keywords: **Synthesis, Nanoclay, Functionalization, Characterization, Antibacterial, Local deposit**

I. INTRODUCTION

A. Synthesis of Novel Materials

The development of novel materials with the ability to inhibit the growth of bacterial and disable them have been of great interest in recent years due to their potential use in everyday products like paints, kitchenware, school and hospital utensils. Recent epidemiological studies have demonstrated a steady increase in infections due to antibiotic-resistant bacteria (Caitlin and Shelley, 2013). The trend in increasing antibiotic resistance demonstrates an ongoing need to develop novel therapeutic treatments for bacterial infections. Inorganic antibacterial agents have several advantages over traditionally used organic agents; like chemical stability, thermal resistance, safety to the user, long lasting action period, low-cost, availability and bio-degradability (Magana *et al.*, 2008). Antibacterial inorganic materials are generally based in metallic ions with antibacterial properties.

According to (Magana *et al.*, 2008) clays, zeolites and other aluminosilicates have been used as carriers with good results because of their high ion exchange capacity, high surface area and sorption capacity, negative surface charge, chemical inertness and low or null toxicity. Some clay minerals have been shown to attract negatively charged bearing bacteria to their surface when dispersed in water. Clay has also been used as adsorbent for non-charged organic molecules like aflatoxins, salicylic acid, herbicides and fungicides. Clays have been used for medicinal applications throughout recorded history. The ancient tablets of Nippur, written approximately 5,000 years ago, listed clays as medicament for healing wounds and stopping ‘‘fluxes from the body’’ (Caitlin and Shelley, 2013). Healing properties of clay have been attributed to the physical and chemical properties of the minerals (Caitlin and Shelley, 2013). Clay minerals have a negative surface charge due to isomorphous substitution that allows the free exchange of particles from the environment such as bacteria, viruses, proteins, nucleic acids, and cations. In particular, kaolinite, talc, and smectite clay minerals are highly absorptive and capable of adhering to the skin, thus offering mechanical protection against external physical or chemical agents and serving as dermatological protectors (Caitlin and Shelley, 2013).

Several methods have been used to modify the common properties of clay (surface area and cation exchange capacity) in order to enhance its performance in different applications. The main effects of these treatments are the collapse of the interlayer and the introduction of structural alterations, diminishing the swelling capacity of the raw clay and modifying the surface charge, respectively. Caitlin and

Shelley, (2013) reported the antibacterial properties of a mixture of natural clay minerals through in vitro antibacterial susceptibility test against a broad spectrum of bacterial pathogens. These clay mixtures showed markedly different antibacterial activity against *Escherichia coli* and methicillin-resistant *Staphylococcus aureus* (MRSA). Some native clay has been reported to exhibit wide spectrum antibacterial activity (Guggeinham and Martin, 1995).

Chemically, clay minerals are hydrous aluminium phylosilicates with variable amount of Iron (Fe), Magnesium (Mg), Alkali metals and other cations found on or near some planetary surface e.g. Kaolinite, **Figure 1**, shows the structure of clay.

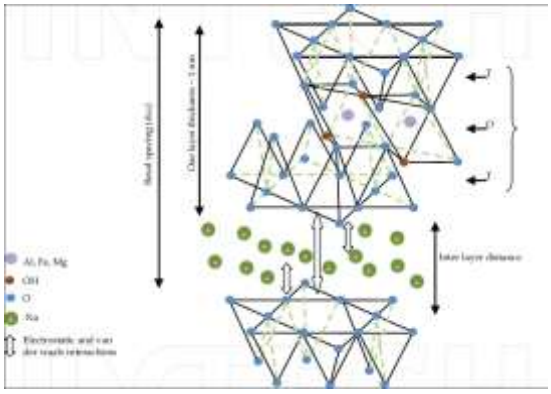

Fig. 1: Structure of clay (Guggeinham and Martin, 1995)

Nanometer scale matter is associated with large surface area for contact attributable to greater fraction of atoms exposed on the surface and its high surface to volume ratio in contrast to its bulk counterpart (Stephen, 2010; Tsagaye, 2012). With these properties, nanoclay could act better than its bulk counterpart in terms of performance as antibacterial agent. Enhanced fire resistance and thermal properties, scratch resistance and dimensional stability, increased mechanical strength and decreased gas permeability and broad-spectrum mycotoxin binding ability. Natural French green clay was reported to heal Buruli ulcer in Ivory Coast-Africa (Figure 2).

Fig.2: Treatment of Buruli ulcer with French green clay (Lynda *et al*., 2008)

The aim of the research was to use amino acids to modify nanoclay because of their biocompatibility and the bactericidal properties of their organo-cations. Functionalization of its surface is thought to enhance surface interaction (s) with bacteria`s carbon skeleton (solubility) while other surface functionalities on amino acids will interact well with those on the surface of the bacteria. Increase in d-spacing is expected to enhance physical adsorption of bacteria and disable them.

II. MATERIALS AND METHODS

All the amino acids used in this work were obtained from a reliable chemical vendor in Nigeria and were BDH chemicals. The clay used was collected from two local mining sites: Dogon-ruwa and Kaffin-koro, denoted as D and K^2 respectively. Other chemicals used include; NaCl, H_2O_2, H_2SO_4, Urea and Thiourea and DMSO obtained from BDH Chemicals. Other are nutrient agar, nutrient broth, Mueller Hinton agar, slant bottles, Cork borer, Wire loop, incubator and petri-dish. Antibacterial profiling of the synthesized nanoclay and modified nanoclay was carried out using Escherichia Coli (E. Coli) Pseudomonas aeroginosa1 (Wound swab), Pseudomonas aeroginosa2 (Ear Swab), Staphylococcus aureus and Proteus Sp. by standard procedure.

A. Collection of Samples

Native clay samples were collected from two different locally mineable locations each in the two selected Local government area of Niger State and these include; Kaffin-koro and Dogon-ruwa in Paikoro and Bosso Local government areas respectively. Native clay sample, 2500 g was weighed and oven-dried for an average period of 24 h at 105 ^oC (Azeh et al., 2016) in order to remove moisture. The sample was taken out of the oven and 2000 g was weighed and placed inside a wooden mortar and ground using a wooden pestle to obtain fine grain particles. The fine clay powder was sieved using an 80 µm standard sieve (Manocha et al., 2008; Azeh et al., 2016). This procedure was repeated for other native clay samples used in this work.

B. Synthesis of Nanoclay from Native Clay Method

Nanoclay was synthesized according to the method described by Chi-kang and Tapei (2010) with slight modifications. In brief, the fine particles of crushed layered clay with size of less than 80 µm, sieved through an 80 mm mesh sieve was mixed with 1:30-500 times by weight of water. The mixture was stirred and allowed to stand still for 24 h for effective hydration to take between the layered clay minerals and water to occur. The suspension was decanted, stirred and allow to stand still for 48 h, where a sediment formed at the bottom of the first decant in a plastic container. This step was repeated, but with addition of 1.0 $moldm^{-3}$ of a saturated solution of sodium acetate followed by treatment with 30 % solution of hydrogen peroxide where sedimentation begins to form at the bottom of the second plastic container and evolution of carbon (iv) oxide, due to the destruction of organic matter in clay. Repeated decantation using deionized water was carried out until the sediment was free of H_2O_2 odour. Finally, the

slurry/liquid free from the slurry was decanted and evaporated at 100-110 ^{o}C to give nanoclay particles. This was used for further treatment and analysis (Azeh et al., 2016).

C. Modification of Native Clay

Nanoclay suspension was firstly saturated with a saturated solution of NaCl and stirred vigorously. From the saturated Na-nanoclay suspension was taken, 250 mL and transferred into a 500 mL beaker followed by the gradual addition of 250 mL solution of each modifier (amino acids) having a pH of 1.8-2.0 and the mixture was stirred on a mechanical stirrer for 1/3 h at ambient temperature. The resulting product was washed until the washed water was free of Cl^- ions (i.e no ppt with $AgNO_3$ solution), drying, grinding, and sieving to get a fine powder of modified nanoclay with various amino acids was achieved (Katti *et al.*, 2010; Pankil *et al*., 2012; Azeh *et al*., 2016).

III. RESULTS AND DISCUSSION

A. Thermal Study of Samples

The thermal degradation studies of the prepared nanoclay and modified products were investigated in order to note the thermal stability of the samples for application purposes. This study is important for the intended applications/uses because the thermal or instability of amino acids has been a speculative subject matter. The reason may be due to lack of comprehensive experimental work on amino acids from the liquid to the decomposition products and the examination of the gaseous products emitted during decomposition. The authors also studied the effects of electrostatic adsorption of amino acids on the nanoclay surface and observe the effect on degradation pattern. In the present study, the modified clay products showed similarities in their decomposition patterns with very little exceptions *(Figures A, B and C).* This observation was attributed to the similarities in the structural resemblances of the amino acids used for the modification of nanoclay. All modified products showed extended thermal stability in the range of 250-450 ^{o}C. This observation was linked to the extended degradation temperature range of the organic modifiers for the external surface modification and the inner surface intercalation respectively. In between this temperature, 250-450 ^{o}C, the modifiers were loss. The decomposition temperature ranges for pure amino acids have been documented to be around 200 – 250 ^{o}C (Wiess et al., 2018). This implies that the initial decomposition temperature recorded around 250-450 ^{o}C, was due to intercalation of the organic cations in between the nanoclay layers coupled with its remarkable fire and heat resistance properties (Al-Juhani, 2015). Similarly, the findings agreed with the work by Yunfei, et al., (2004) on the organic intercalation of MMT, where they found extended decomposition temperature in the range of 178 -358 ^{o}C for the MMT intercalated with octadecyl trimethylammonium bromide. It was concluded that the protection of the organic modifiers by the layer sheets resulted in the increase in initial thermal degradation of the organoclay products. The volatile products are NH_3, CO_2 and CO, which may be due to the presence of N-terminal amine and the α-carbonyl groups. The decomposition peak around 150-200 ^{o}C is assigned to unbound water molecules in clay, similar to the documented work by Osabor et al., (2016) and Boumediene et al., (2016). The decomposition recorded in the range of 450-600 ^{o}C (D'mello, 2003; Osabor et al., 2016) was due to bound water molecules in between the nanoclay layers, resulting from the dehydroxylation of the inner –OH group in kaolinite minerals. Yunfei, et al., (2004) reported this around 556 – 636 ^{o}C, due to dehydroxylation of the inner –OH group. At 600-750 ^{o}C more nitrogen-containing volatile derivatives are expected from the aromatic amino acids as a result of the high temperature required to pyrolyze especially, the N-cyclic side chain of tryptophan to produce ammonia. This observation was similar to the findings by Liu et al., (2016) on the pyrolysis of amino acids. The characteristics exhibited by the nanoclay materials make them potential candidates for use as adsorbents and/or for the melt processing formulation of nanocomposites. Meshal et al., (2017) observed increase in the values of thermal degradation of MMT modified with two different cationic organic modifiers. They attributed the increase in the values of thermal stability of the nanocomposites formulated, to the addition of the cationic modifiers and the clay interlayer ability to trap the volatiles, and preventing their escape from the matrix of the nanocomposites**.** Decomposition temperature recorded in the at 800^{o}C, and above was due to inorganic char residue, resulting from the nanoclay component of the products synthesized, and the process is exothermic in nature (Osabor et al., 2009; 2016). The thermal decomposition ranges for the aromatic amino acids recorded around 372 – 496 ^{o}C and 374 – 465 ^{o}C were for phenylalanine and tryptophan analogues respectively. The findings in this work closely relates to the work documented by Kato et al., (1971) on the pyrolysis of amino acids and subsequent study of the volatiles using gas chromatography by Kamata and Masko and the findings by Boumediene et al., (2016) on the thermal degradation of ionic liquid in organo-modified bentonite around 30^{o}C. The maximum temperature for the pyrolysis of the aromatic amino acids in this work was slightly higher than that reported by Kamato and Masko (Kato et al., 1997). The researchers have attributed the extended degradation temperature in the present study to the protective properties of nanoclay layer sheets. At these temperatures, different volatile compounds are produced. Based on the findings by Kato et al., (1971), phenols and indole are produced by the pyrolysis of phenylalanine and tryptophan at 300 ^{o}C. It could be seen that the TGA peaks significant to the degradation pattern of the aromatic ones was extended, and the reason being that the nanoclay insulated the organo-cations between its layer sheets. Thus, the observed increased in the degradation pattern.

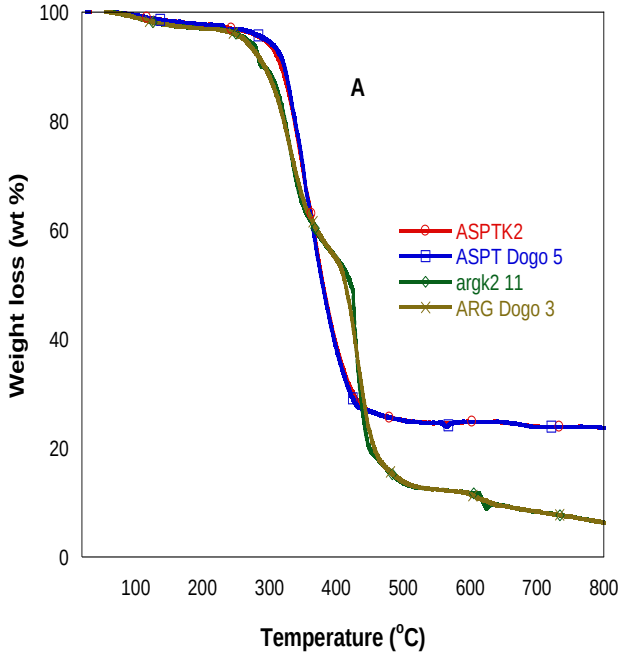

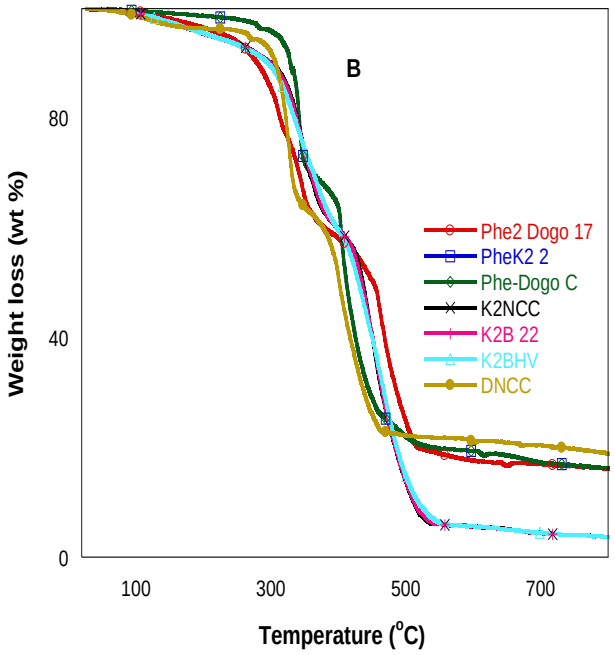

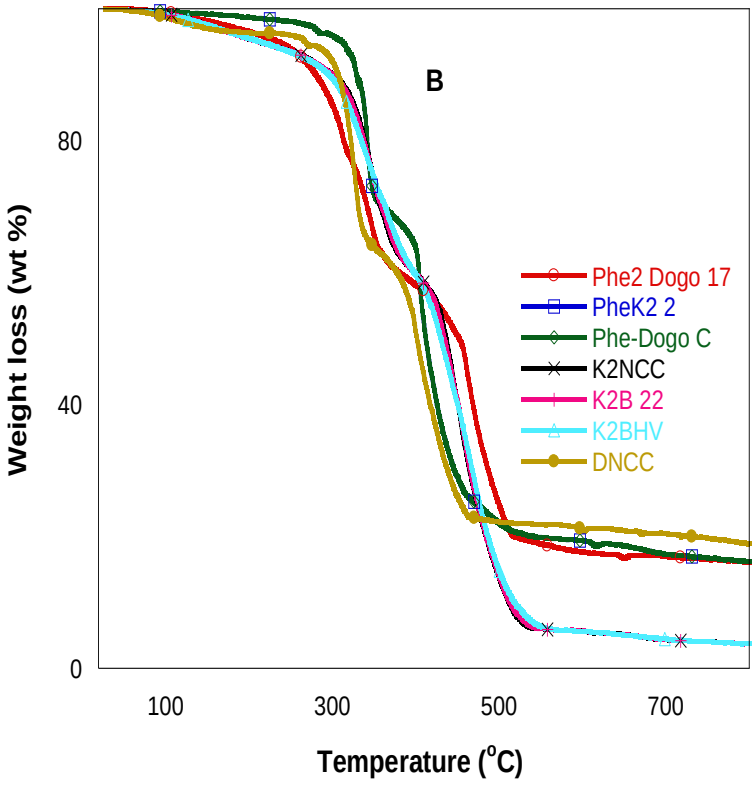

Figs. A, B and C: TGA of Modified Nanoclay and Control

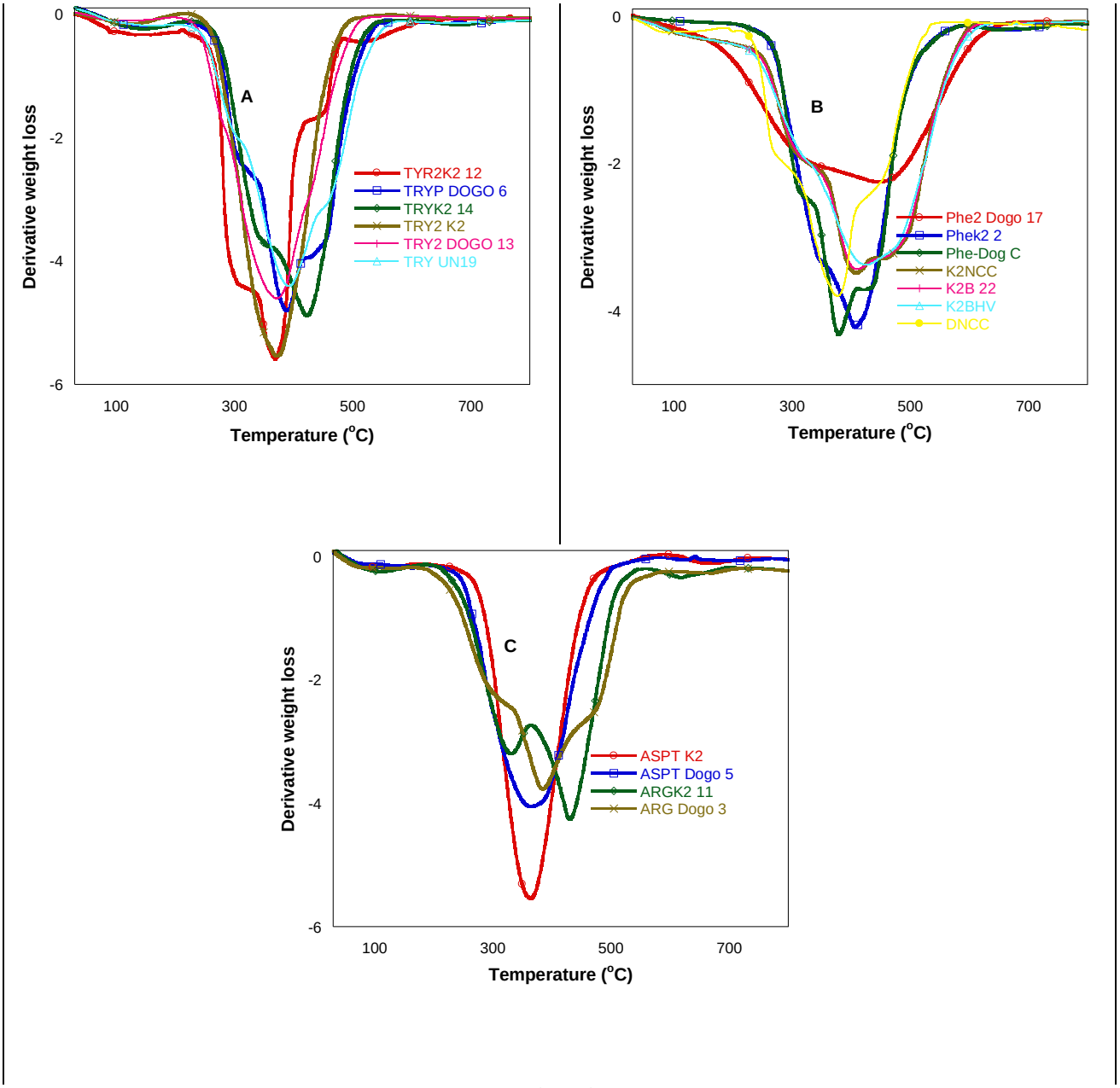

Figs. A, B and C: DTGA of Modified Nanoclay and Control

B. Raman Spectroscopy Study of Samples

Raman spectroscopy increasingly finds utilization for its ability to characterize small sample, it's a non-destructive rapid technique for the analysis of paints, inks, fibres, mineral residues, pharmaceuticals etc.

C. The region below <200 cm^{-1}

The Raman spectral data and band assignment of the nanoclay and modified samples are shown in *Figures A, B* and *Table 1* respectively. The Raman spectral peaks of the two clayey materials analysed (Dogon ruwa and Kaffin-koro clay) showed similarities in their peak band. The observed peaks in the lower region of <200 cm^{-1} was found around 158-160 cm^{-1} irrespective of the treatment of the samples. The presence of the spectral absorption peaks at 158 and 160 cm^{-1} has been shown to be a good evidence of the presence of clay minerals (Frost, 1995; Natalia et al., 2013; Bhaskar et al., 2016). This band has been assigned to O-AL-O bend vibration due to kaolinite mineral (Frost, 1995; Saikia et al., 2016). These bands are similar and are therefore, due to Raman shift from 158 to 160 cm^{-1}. In addition, the band also indicates the

presence of brookite in the studied clay minerals, similar to the findings by Enver, (1997), who observed the band at 155 cm^{-1}. This implies that there are similarities in the geochemical formation of the clay collected at Kaffin-koro and Dogon-Ruwa in Niger State respectively. The weak absorption peak around 248-262cm^{-1} was ascribed to SiO_4 (quartz) tetrahedral structure (Caterina et al., 2003; Thiago et al., 2017; Frank, 2018). The peak which occurred at 248 and 250cm^{-1}, due to symmetry stretch of Si-O, was similar in all the samples. Thus, the peak at 248 cm^{-1} might be due to Raman shift as it appeared at higher absorption band, 250 cm^{-1} assignable to Si-O for silicates (Janice and Enver, 2004; Natalia et al., 2013; Saikia et al., 2016; Frank, 2018). The medium band at 262 cm^{-1}, which appeared in all the samples, showed similarities in its intensity. This peak is a doublet typical of the presence of different glassy minerals, such as basaltic, quartz, goethite, hematite and magnetite in the nanoclay samples. The occurrence of this band a little below the typical hematite band at 283 and 293 cm^{-1} (Natalia et al., 2013), may be due to the presence of intercalates/modifiers in clay layers. The band around 396-398 cm^{-1} was substantially a medium peak found in all samples, similar to the findings by Clifford et al., (1985) in the study of Kaolinite native clay in aqueous suspensions. The bands at 396 and 398 cm^{-1} agreed with the findings by (Natalia et al., 2013), who reported the appearance of the peaks closely to the absorption peaks at 414 and 417 cm^{-1} in natural goethite, a glassy (SiO_2) clay mineral.

The unique Raman bands which appeared at 396 and 398 cm^{-1} are medium peaks whereas, the band around 414-416 cm^{-1} were very strong Raman band significant to the presence of silica polymorphs (quartz, crystallite, tridymite and opal) in all nanoclay and nanoclay modified (Mikhail et al., 2005; Palanivel and Velray, 2007; Natalia et al., 2013; Rodica-Mariana et al., 2016; Saikia et al., 2016). These band are assigned to Si-O-Si and Si-O (Kaolinite/Goethite) bends vibrational modes. The bands around 612, 636 and 638 cm^{-1} are due to the presence of feldspar/hematite resulting from Si-O-Si bend (Natalia et al., 2013). Clifford et al., (1985), reported the observance of this bands at 637 cm^{-1} in Kaolinite clay mineral while the band at 612 cm^{-1} was reported by Natalia et al., (2013) in volcanic ash. Similarly, Enver, (1997), reported the presence of this peak in Kaolin. The band from 752 – 762 cm^{-1} was a clear indication of the presence of kaolinite mineral, due to AL-O-Si and tetrahedral SiO_4 stretch vibrations similar to the findings by Janice and Enver, (2004); Saikia et al., (2016). This indicates that the clay samples collected at different locations are significantly rich in Kaolinite minerals.

The band recorded around 801 – 820 cm^{-1} are medium bands ascribed to Al-O-Si bend, due to the mineral phases, Illite or Kaolinite. This band was reported by Saikia et al., (2016) in the range of 790-792 cm^{-1} in native clay and at 750 cm^{-1} and at higher mode at 806 cm^{-1} by Frank Friedrich, (2004). In this work its occurrence at 801-820 cm^{-1}, resulted from Raman shift due to modification. This band was found in two modified samples, TRPDogo and K^2B22. Another specific band, which appeared distinguished from other mineral phases was the band at 842 and 844 cm^{-1} respectively in both modified and controlled samples, due to wagging/strong distortion vibration mode of Al-O-H and Mg-O-H, resulting from the -OH bonded with the octahedral metal ions in Al-Mg-OH. These are medium bands and indicates the presence of mineral phases such as Illite/Montmorillonite (Saikia *et al.*, 2016) and halloysite and montmorillonite clay mineral reported by Mikhail et al., (2005) and Maria et al., (2020). In addition, the band was in agreement with the findings by Natalia et al., (2013) on volcanic ash respectively. The Raman band at 866 cm^{-1}, observed in all the samples was a clear indication of the presence of different types of clay mineral present in the studied clay deposit in Niger State. The weak band at 904 cm^{-1} has been assigned to -OH deformation in Kaolinite or Montmorillonite. This peak usually will appear around 940 and 915 cm^{-1} for the inner surface and inner sheet hydroxyls. However, the appearance of the band at low frequency, 904 cm^{-1} for the tryptophan modified sample may be due to Raman shift of 915 cm^{-1}, resulting from the disorder caused by the interference of the –N-H group of the indole side-chain of tryptophan. This kind of effect has been reported by D'mello, (2003) on native clay intercalated with hydrazine molecules. The band around 1002-1004 cm^{-1} was ascribed to the Si-O stretch vibration similar to the findings by Frank, (2004).

The high and intense Raman band observed around 1774 – 1782 cm^{-1} was ascribed to νC=O stretch vibrational frequency of the amide groups. Raman absorption peak for the Y-caprolactone carbonyl (C=O) around 1766 – 1869 cm^{-1} was reported by Wenwen et al., (2017). The appearance of this band in the amino acid-modified samples was a clear indication that intermolecular interaction occurred right inside the nanoclay layer. This implied that the nanoclay layers were not only functionalized by the organic cations, but this layers also served as potential platforms or vessels for the synthesis of proteins, due to dimerization of amino acid monomers in the nanoclay layers. This was evidenced by the intense absorption peak in the range of 1774-1784 cm^{-1}, resulting from carbonyl (C=O) coupling vibrational frequency of the amide carbonyl linkage. The non-appearance of this peak in all non-organic modified clay minerals analysed was good evidence of the presence of organic modifiers and indicates the success of modification. The peak absorption indicative of the organic intercalates appeared around 2900 – 3001 cm^{-1} in all modified samples. The absorption band was ascribed to the symmetry stretch vibration of $–CH_2$ of the organic modifiers. This implies the success of cationic modification of nanoclay. Wenwen *et al*., (2017), reported the vibrational frequency for the of $–CH_2$ stretching mode around 2983 – 2939 cm^{-1}.

The Raman study of the clay samples and their modified products with bands in the region of 158-1002 cm^{-1}, suggested the presence of different types of non-crystalline (glassy-type) silicates clay minerals in the native clay collected at Kaffin-Koro and Dogon-Ruwa respectively.

Table 1: Raman Peak Assignment (cm^{-1}) of Samples and Chemical Phases in Clay Minerals

K^2NCC	K^2B22	ARG-DOGO3	ARG-$K^2$11	ASPT-DOGO5	ASPT-K^2	TRYP-DOGO6	TRYP-K^2-14	TYPT UN-19	Assignment	Chemical phases
-	158	158	-	158	158	158	158	158	O-Al-O	Kaolinite
160	-	-	160	-	-	-	-	-	O-Al-O	Brookite
-	-	248	-	-	248	248	-	-	SiO_4	Quartz
250			250	250	-	-	250	250	SiO_4	Quartz
262	262	262	262	262	262	262	262	262	SiO_4	Quartz
-	352	-	-	-	-	-	-	-	SiO_4	Quartz
-	-	-	-	-	-	-	396	-	Al-O-Si/TiO_2	Kaolinite/ goethite/Anatase
398	398	398	398	398	398	398	-	398	Al-O-Si/TiO_2	Kaolinite/ goethite/Anatase
-	414	414	-	414	414	-	414	414	Si-O-Si and Si-O	quartz, crystallite, tridymite and opal
416	-	-	416	-	-	416	-	-	Si-O-Si and Si-O	quartz, crystallite, tridymite and opal/Kaolinite
-	-	-	-	-	612	-	-	-	Si-O-Si bend	Feldspar/ Kaolinite
-	636	636	-	636	636	636	636	636	Si-O-Si bend	Feldspar/ Kaolinite
638	-	-	638	-	-	-	-	-	Si-O-Si	Feldspar/ Kaolinite
-	-	-	-	-	-	-	-	752	AL-O-Si str	Kaolinite
-	-	-	-	-	-	-	-	762	AL-O-Si str	Kaolinite
-	-	-	-	-	-	801	-	-	AL-O-Si	Kaolinite/Illite
	802								AL-O-Si	Kaolinite/Illite
-	-	-	-	-	818	-	-	-		
-	842	842	-	842	842	-	842	842	Al-OH, Mg-OH	Illite/ halloysite and montmorillonite
844	-	-	844	-	-	-	-	-	Al-OH, Mg-OH	Illite/ halloysite and montmorillonite
866	866	866	-	866	866	866	866	866	Al-OH, Mg-OH	Illite/ halloysite and montmorillonite
-	-	-	868	-	-	-	-	-	Al-OH, Mg-OH	Illite/ halloysite and montmorillonite
-	-	-	-	-	-	-	904W	-	-OH	Kaolinite/Montmorillonite
1002	1002	1002	1002	1002M	1002	1002	1002	1002	Si-O	
-	-	-	1004	-	-	-	-	-	Si-O	
-	-	-	1774	-	-	-	-	-	C=O	Amide carbonyl polymer
-	-	-	-	-	1780	-	-	-	C=O	Amide
1782S	1782	1782	-	1782	1782S	1782S	1782	1782	C=O	Amide
-	-	-	1784	-	-	-	-	-	C=O	Amide

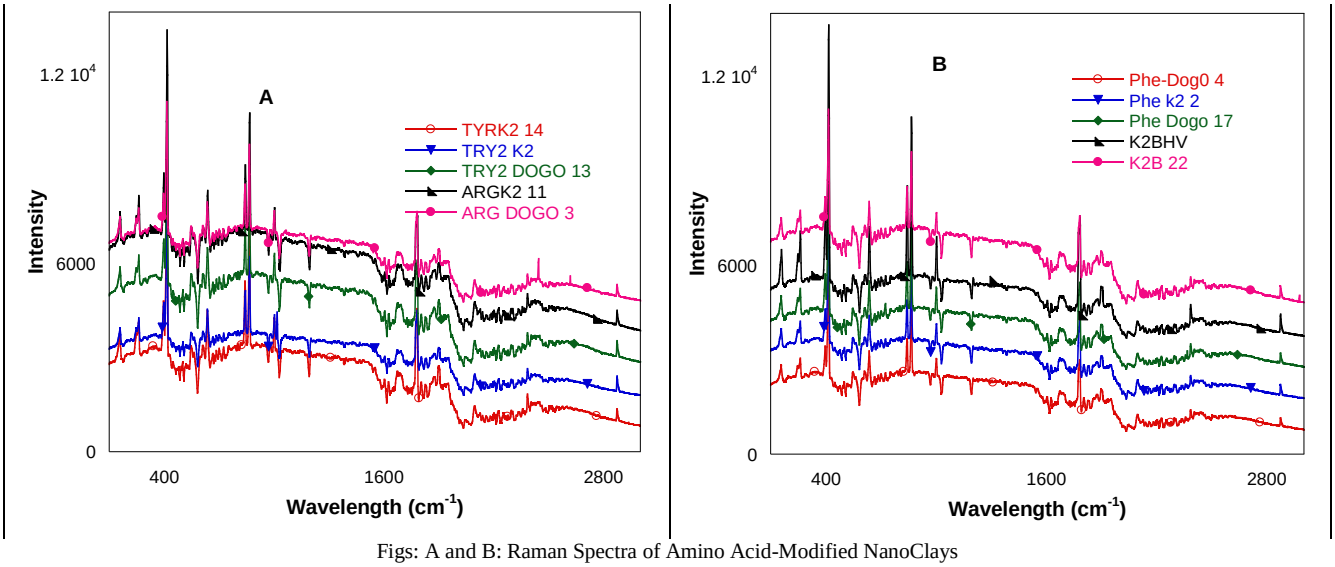

Figs: A and B: Raman Spectra of Amino Acid-Modified NanoClays

D. BET and Particle Size Analysis

The BET analysis of nanoclay samples was determined using nitrogen adsorption isotherm (Adsorption/Desorption). Results show that the BET_{SA} for the control sample denoted as Dogon-ruwa nanoclay control (DNCC), was 432.6 m^2/g. This was far larger than values reported for different clay and clay products (Felix et al., 2011; Utpalendu and Manika, 2013; Yilmaz et al., 2019; Emeka et al., 2017). Modification with the organo-cations (Phe^+ and Arg^+) decreased the surface area, similar to the findings by Mallakpour and Dinari, (2011), on new organoclays using natural amino acids and cloisites Na^+. Surface coverage was calculated as 28.3 % and 76.4 % respectively *(Table 2)*. Raman data show that the clays being investigated were composed of mixed-layer clay minerals and BET values obtained were in the range of 102.1 - 432.6 m^2/g. Clay minerals with values greater than 100 m^2/g have been reported to be composed of mixed-layers (Meral et al., (2017). The results are significant for applications in biomolecule adsorption.

Table 2: BET Surface Area of Nanoclay and Modified Nanoclay Samples

Representative Sample	BET Surface Area (m^2/g)	Surface Coverage (%)
DNCC	432.6	100
Phe Dogon-ruwa	310.3	28.3
ARGDogon-ruwa	102.1	76.4

The particle size distribution histogram shows that DNCC sample had particle diameter in the range of 200-400 nm while the particle size of the modified samples was in the range of 200-900 nm and 300-800 nm, for Arg^+Dogo3 and Phe^+Dogon-ruwa *(Figures c, d and e)* respectively. The increase in the particle size of the modified samples was attributable to the surface and interlayer adsorption of the organic modifiers. This was expected as a result of the increase in d-spacing. In addition, the increase in the particles could be due to the formation of proteins, resulting from build-up of the amide linkage through $–NH_2$ and -COOH interactions on clay layers, which served as templates for protein synthesis.

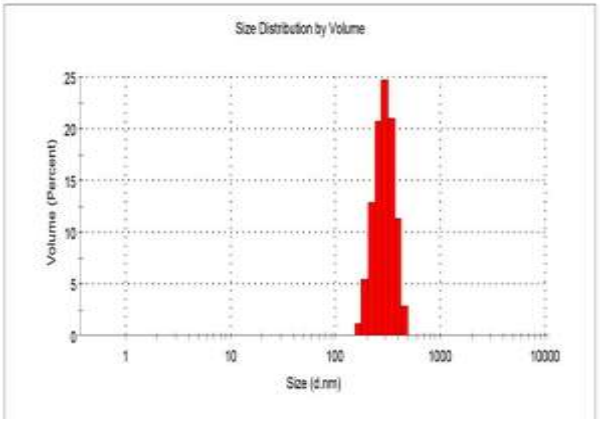

Fig. C: Particle size distribution intensity for DNCC Sample

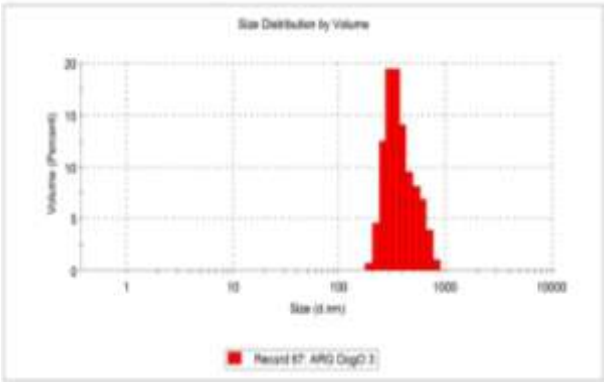

Fig. D: Particle size distribution intensity for ARGDOGO3 Sample

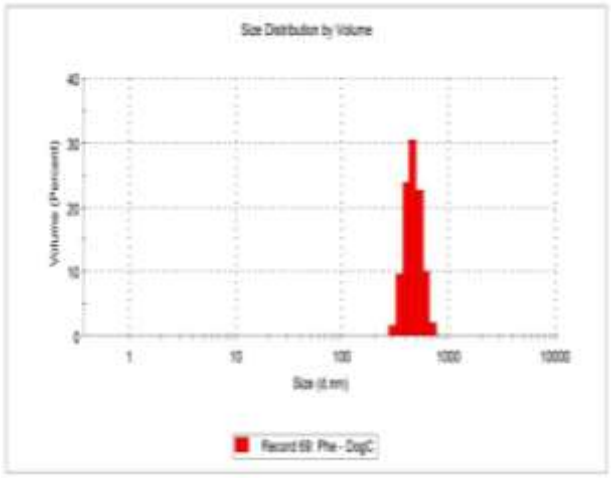

Fig. E: Particle size distribution intensity for PheDOGO Sample

E. Modified Nanoclay Exhibit Variable in Vitro Antibacterial Activities

The susceptibility, minimum inhibitory (MIC) and the Minimum Bacteriostatic concentration of Nine (9) samples were investigated against five organisms and a standard drug, Ampiclox. The organisms were clinical isolates and include; Escherichia Coli, Pseudomonas aeruginosa (wound swab), Pseudomonas aeruginosa (Ear swab), Staphylococcus aureus, and Proteus Sp. Zone of Inhibition of the nanoclay and its modified products is as shown in *(Table 3).* With the various modifiers used, the modified products exhibited different degrees of inhibitions against the organisms under investigation. The susceptibility of the organisms to the different clay products range from and this ranged from 12-26 mm zone of inhibition as against 26-31 mm of the standard drug. This was a clear indicator of the robust antibacterial activity of the modified nanoclay samples. The control sample designated as DNCC (Dogon-ruwa Nanoclay Control) showed no activity against any of the test organisms. The inability of the control sample (DNCC) could mean that the sample from Dogon-ruwa is not naturally healing clay similar to the report on some French clay by Lynda et al., (2011). However, modification with amino acid imparted appreciably good antibacterial activity on the clay.

The activity of the modified samples could be attributable to the electrostatic adsorption of organo-cations onto the nanoclay surface and the presence of surface functional groups (–OH, -NH, $-NH_2$, -CO, -COOH, -SH, and –C-N-), which were evidenced by Raman Spectroscopic and TGA data, similar to the findings by Azeh et al., (2020) on cellulose acetate nanocomposite films. Due to the tendency formation of metal complexes between the organocations and metals present in clay, the antibacterial properties of the modified samples could be linked to the formation of metal complex species and especially, those involving alpha amino acids are known for their ability to inhibit the growth of bacteria (Zahid et al., 2006: Yuichi, Masako and Osamu, 2009). The presence of lone-pair species on could enhance interaction which could leach-out the critical cell contents and eventual disability on the part of the organism. Metal ions such as Fe^{2+}, Zn^{2+}, Cu^{2+} and the presence of Phosphorus have been reported as modulating metal species with high potential for killing and/or disabling microorganisms (Lynda et al., 2011; Caitlin et al., 2013).

Table 3: Zone of Inhibition (mm) of Clinical Isolates by Modified Nanoclay Samples

Susceptibility Test	DNCC21	PheD4	TRY2D4	TRY2D15	TRY2D13	ARGD3	ASP2D8	Phe2D17	TRYUN19	Ampiclox
Escherichia Coli	NA	NA	NA	NA	16	18	17	19	12	26
Pseudomonas aeroginosa1	NA	NA	NA	19	NA	NA	NA	NA	NA	31
Pseudomonas aeroginosa2	NA	18	23	NA	18	NA	26	NA	NA	28
Staphylococcus aureus	NA	NA	NA	NA	NA	19	NA	NA	21	NA
Proteus Sp.	NA	19	NA	NA	21	18	22	NA	NA	NA

The minimal inhibitory concentration (MIC) *(Table 4)* of the various modified nanoclay samples ranged from 12.5-100 mg/mL, closely related the MIC value for the standard drug, Ampiclox (12.5-25 mg/mL). It is worthy note that some modified samples showed competitive minimal inhibitory activity with the standard drug. Samples ASPD8 with MIC of 12.5 mg/mL to inhibit the growth of Proteus Sp., similar to the lowest MIC of the standard drug and the MIC of 25 mg/mL exhibited by ArgD3, against Staphylococcus aureus equivalent to that of the standard drug. TyroD13 had 25 and 50 mg/mL against Proteus sp. And Pseudomonas aeroginosa2 (Ear swab). This result is significant for the pharmaceutical formulation of tropical gels and suspension with potential for the treatment of ailments caused by these organisms.

Table 4: Minimal Inhibitory Concentration (MIC) mg/mL of Clinical Isolates by Modified Nanoclay/Control Samples

Susceptibility Test	DNC C21	PheD 4	TRY2 D4	TRY2 D15	TRY2 D13	TRYD 6	ARGD3	ASP2 D8	Phe2D 17	TRYU N19	Ampiclox
Escherichia Coli	-	-	-	-	100	-	50	100	50	100	25
Pseudomonas aeroginosa1	-	-	-	50	-	100	-	-	-	-	12.5
Pseudomonas aeroginosa2	-	100	50	-	50	-	-	12.5	-	-	12.5
Staphylococcus aureus	-	-	-	-	-	-	25	-	50	50	25
Proteus Sp.	-	50	-	-	25	100	50	50	-	-	12.5

The minimal bacteriostatic concentration (MBC) *(Table 5)* for the modified nanoclay materials ranged from 12.5 – 100 mg/mL whereas, the value obtained for the standard drug was 12.5-50 mg/mL. Both the modified samples and the standard drug showed comparable performance in terms of the complete elimination of the bacteria. This implies that the minimum concentration of the modified samples required for the complete elimination of test organisms by the clay samples being evaluated were 12.5, 50.0 and 100 mg/mL respectively. This is an indication of the potentials of the modified samples to disable the growth of certain bacteria pathogens that are dangerous to human health. Research has shown that not all clay deposits are antibacterial in nature (Lynda et al., 2011).

Table 5: Minimal Bacteriostatic Concentration (MBC) mg/mL of Clinical Isolates by Modified Nanoclay/Control Samples

Susceptibility Test	DNCC21	PheD4	TRY2D4	TRY2D15	TRY2D13	TRYD6	ARGD3	ASP2D8	Phe2D17	TRYUN19	Ampiclox
Escherichia Coli	-	-	-	-	100	-	50	100	50	100	25
Pseudomonas aeroginosa1	-	-	-	50	-	100	-	-	-	-	50
Pseudomonas aeroginosa2	-	100	50	-	50	-	-	12.5	-	-	12.5
Staphylococcus aureus	-	-	-	-	-	-	25	-	100	50	25
Proteus Sp.	-	50	-	-	25	100	50	50	-	-	12.5

IV. ACKNOWLEDGEMENTS

The authors gratefully acknowledge IBB University IBR TETfund Research 2018-2019 Intervention awarded in 2019, for the financial support, which ensured the success of this research work.

CONFLICT OF INTEREST

The authors declared that no conflict of interest exists.

REFERENCES

[1] Al-Juhani, Abdulhadi A. (2015). Rheology, mechanical properties, and thermal stability of maleated polyethylene filled with nanoclays. *Journal of Nanomaterials,* 2015, 1-11.

[2] Pankil, S., Rajeev, M. and Siddh, N. U. Y. (2012). Clay modification by the use of organic cations. Green and Sustainable Chemistry, 2, 21-25.

[3] Azeh, Y., Olatunji, G. A., Mohammad, Y. S., Agwuncha, C. S., Abubakar, A., Damilare, O. S. and Tanko, U. M. (2016). Application of Ft-Ir and scanning electron microscopy for characterization of modified nanoclay using selected amino acids. ***Lajans,*** 1(1), 111-119.

[4] Boumediene, H., Didier, V., Karima, D., Habib, B., Taqiyeddine, M., Serge, B., Ahmed, H. and Mustapha, R. (2016). Preparation and thermal properties of organically modified bentonite with ionic liquids. *ChemXpress*, 9(4), 295-302.

[5] Bhaskar, J. S., Parthasarathy, G., Borah, R. R. and Borthakur, R. (2016). Raman and FTIR spectroscopic evaluation of clay minerals and estimation of metal contaminations in natural deposition of surface sediments from Brahmaputra River. *International Journal of Geosciences*, 7, 873-883.

[6] Clifford, T. J., garrison, S. and Robert, R. B. (1985). Raman spectroscopic study of kaolinite in aqueous suspension. *Clays and Clay Minerals,* 33 (6), 483-489.

[7] Chi-Kang, L., Taipei, T.W. (2010). Pure nanoclay and process for preparing nanoclay, *Journal of nanotechnology*, 1, 1-10.

[8] Catherina, and Daniela, g. (2003). Characterization of chrysotile, antigorite and lizardite by ft-raman spectroscopy. *The Canadian Mineralogist*, 41, 883-890.

[9] Caitlin, C. O. and Shelley, E. H. (2013). Exchangeable ions sre responsible for the in vitro antibacterial properties of natural clay mixtures. *Plos One*, 8 (5), 1-9.

[10] Enver, M. (1997). Identification of minor amounts of anatase in kaolins. *American Mineralogist, Raman spectroscopy*, 82, 203-206.

[11] Emeka, T. N., Casimir, E. G., George, I. N., Adamu, K. I. and Yilleng, M. T. (2017). Morphological and microstructural characterization of organoclays from low smectite containing clays materials. *Chemical Science International Journal*, 18(1), 1-17.

[12] Frank Friedrich (2004). Spectroscopic investigations of delaminated and intercalated phyllosilicates Zur Erlangung des akademischen Grades eines DOKTORS DER Naturwissenschaften von der Fakultät für Bauingenieur-, Geo- und Umweltwissenschaften der Universität Fridericiana zu Karlsruhe (TH) genehmigte dissertation von Diplom-Mineraloge aus Mannheim Tag der mündlichen Prüfung.

[13] Felix, M., Karin, Eusterhues, G. J. P, Kai, U. T. (2011). Specific surface area of clay minerals: Comparison between atomic force microscopy measurements and bulk-gas (N) and -liquid (EGME) adsorption methods. ***Applied Clay Science,*** 53(1), 20-26.

[14] Guggeinheim, S. and Martin, R. T. (1995). Definition clay and clay mineral: Joint Report of the AIPEA nomenclature committees. ***Clay and clay miner.***, 43(2), 255 - 256.

[15] Lynda, B. W., Shelley, E. H., Rossman, F. G. Jr. and Dennis, D. E. (2008). Chemical and mineralogical characteristics of french green clays used for healing. ***Clays Clay Miner.***, 56(4), 437–452.

[16] Lynda, B. W., David W. M., Dennis, D. E., Ronald, W. H., Amanda, G. T., Panjai, P. and Amisha, T. P-P. (2011). What makes a natural clay antibacterial? ***Environ. Sci. Technol.***, 45(8), 3768–3773.

[17] Meral, D., Umran, D. A., Irem, Y. F., Dogan, A., Ira, B. and Dale, E. W. (2007). Baseline studies of the clay minerals society special clays: Specific surface area by the Brunauer Emmett Teller (BET) method. Clays and Clay Minerals, 55, 534–54.

[18] Manocha, S., Nikesh, P. and Manocha L. M. (2008). Development and characterization of nanoclays from indian clay. ***Defence science journal,*** 58, 517-524.

[19] Meshal, A., Jacob, S., Fatema, A. and Gils, A. (2017). Comparative effects of MMT clay modified with two different cationic surfactants on the thermal and rheological roperties of Polpypropylene nanocomposites. *International Journal of Polymer Science*, 1-8.

[20] Mikhail, O., Victor, H. G. M. and Alise, S. (2020). Mineralogical and geochemical studies of hardened subsurface layers in soils of the Azufres and Atecuaro volcanic calderas, southwestern Mexico. *Can. J. Soil.* ***Sci.*** 197.210.85.171 on 04/01/20.

[21] Natalia. P. I., Susanne, H., Bernadett, W., Reinhard, N., Christoph, H. and Thomas, B. (2013). Identification and characterization of individual airborne volcanic ash particles by Raman micro spectroscopy. *Anal Bioanal Chem.*, 405, 9071–9084.

[22] Rodica-Mariana, I., Radu-Claudiu, F., Sofia, T., Irina, F., Ioana-Raluca, B., Daniela, Ţ-C. and Mihaela-Lucia. I. (2016). Ceramic materials based on clay minerals in cultural http://dx.doi.org/10.5772/61633.

[23] Stephen, J. E. (2010). Cellulose nanowhiskers: Promising materials for advanced applications. DOI: 10.1039/c0sm00142b.

[24] Tsegaye, G. A. (2012). Exploring potential environmental applications of selenium nanoparticles. Thesis submitted in partial fulfilment of the requirements for the joint academic degree of International Master of Science In Environmental Technology and Engineering, Ghent University (Belgium), Ictp (Czech Republic), Unesco-Ihe (The Netherlands).

[25] Thiago, G. C., Marcelino, D., Correia, M., Lucas, B. R., Sailer, S. S., Juliana, S. M., Lucas, B., Isabela, D. S. M. (2017). Spectroscopic characterization of recently excavated archaeological potsherds of Taquara/Itararé tradition from Tobias Wagner site (Santa Catarina – Brazil) (2017). *Journal of Archaeological Science*: Reports 12, 561–568.

[26] Utpalendu, K. and Manika, P. (2013). Specific surface area and pore-size distribution in clays and shales. *Geophysical Prospecting*, 61, 341–362.

[27] Wenwen, X., Yanfang, S., Xiaoping, D., Si, L., Huigan, W., Jiadan, X. and Xuming, Z. (2017). Local order and vibrational coupling of the C=O Stretching Mode of γ-Caprolactone in liquid binary mixtures. Scientific Reports, 7, 12182; DOI:10.1038/s41598-017-12030-1.

[28] Yunfei, X., Zhe, D., and Ray L. F. (2004). Structure of organo-clays: An X-ray diffraction and Thermogravimetric analysis study. *Journal of Colloid and Interface Science*, 277(1), 116-120.

[29] Yuichi Shimazaki, Masako Takanib and Osamu Yamauchi (2009). Metal complexes of amino acids and amino acids side chain groups: Structure and properties. Dalton Transactions, (38), 7854-7869.0]. Yilmaz, B., Irmak, E. T., Turhan, Y.,

[30] Dogan, S., Dogan, M. and Turhan, O. (2019). Synthesis, characterization and biological properties of intercalated kaolinite nanoclays: Intercalation and biocompatibility. *Advances in Materials Science*, 19(1), (59), 83-99.

[31] Zahid, H. C., Arif, M., Muhammad, A. A. and Claudiu, T. S. (2006). Metal-Based Antibacterial and Antifungal Agents: Synthesis, Characterization, and In Vitro Biological Evaluation of Co(II), Cu(II), Ni(II), and Zn(II) Complexes With Amino Acid-Derived Compounds. Bioinorganic Chemistry and Applications, Vol. (2006), 1–13; DOI 10.1155/BCA/2006/83131.

ABBREVIATIONS

$ASP2K^2$:

Aspartame Kaffin-koro Modified Nanoclay

ASP2D8: Aspartame Dogon-ruwa Modified Nanoclay

ASPD5: Aspartame Dogon-ruwa Modified Nanoclay

$PheK^2$: Phenylalanine Kaffin-koro Modified Nanoclay

Pke2D17: Phenylalanine Dogon-ruwa Modified Nanoclay

PheD4: Phenylalanine Dogon-ruwa Modified Nanoclay

TYRD1: Tyrosine Dogon-ruwa Modified Nanoclay

TYRD15: Tyrosine Dogon-ruwa Modified Nanoclay

TYRD13: Tyrosine Dogon-ruwa Modified Nanoclay

TYRUn19: Tyrosine Unprotonated Modified Nanoclay

DNCC: Dogon-ruwa Nanoclay Control

K^2NCC20: Kaffin-koro Nanoclay Control

TRY2D4: Tryptophan Dogon-ruwa Modified Nanoclay

TRYPD6: Tryptophan Dogon-ruwa Modified Nanoclay

K^2BH4: Kaffin-koro Bleached H_2SO_4 Nanoclay

AGRD3: Arginine Dogon-ruwa Modified Nanoclay

$ARGK^2$: Arginine Kaffin-koro Modified Nanoclay

$TYRK^2$14: Tyrosine Kaffin-koro Modified Nanoclay

$TYR2K^2$: Tyrosine Kaffin-koro Modified Nanoclay

$TYRK^2$16: Tyrosine Kaffin-koro Modified Nanoclay

K^2B: Kaffin-koro Bleached Nanoclay

Ampiclox: Ampicloxacine